Case Studies in Thermal Engineering 10 (2017) 234–243

Contents lists available at ScienceDirect

Case Studies in Thermal Engineering

journal homepage: www.elsevier.com/locate/csite

Experimental study of flow through compressor Cascade

Satyam Panchal[a,*], Vijay Mayavanshi[b]

[a] Mechanical and Mechatronics Engineering Department, University of Waterloo, 200 University Avenue West, Waterloo, Ontario, Canada N2L 3G1
[b] Mechanical Engineering Department, Faculty of Engineering and Technology, The Maharaja Sayajirao University of Baroda, Baroda 390001, Gujarat, India

ARTICLE INFO

Keywords:
Cascade
Aerofoil blade
Incidence
Deflection
Static pressure
Pressure probe
Flow separation

ABSTRACT

The objective of this research work is to study the behaviour of flow at the inlet, within the blade passage and at the exit of a compressor cascade. For this purpose, a cascade with six numbers of aerofoil blades was designed and constructed. The cascade was fitted on the cascade test tunnel. Out of six blades two were instrumented for measuring the pressure distribution on the pressure and suction surface. The blades had a parabolic camber line, with a maximum camber position at 40% of the chord from the leading edge of the blade. The profile of the blade was C4, height of the blade was 160 mm, chord length was 80 mm, camber angle was 45° and stagger angle was 30°. Similarly, the length of the cascade was 300 mm, span was 160 mm, pitch was 60 mm, the actual chord of the cascade was 80 mm, the axial chord of the cascade was 70 mm, the stagger angle of the cascade was 30° and the pitch-chord ratio was 0.75. The data was taken and analyzed at −500% of the axial chord before the cascade, −25% of the axial chord before the leading edge, 25%, 50%, 75% and 150% of the axial chord from the leading edge of the blade. The readings were taken from the cascade wall to the mid span position along the pitch wise direction. The angle of incidence was also changed during the experiment and varied from i = −50°, −30°, −10° to 5°.

1. Introduction

The effectiveness of jet engines has been halved during the last thirty years, thanks in part to more effective turbine and compressor blade design methods [1]. These methods were improved by experimental verification. Experience shows that experiments are indispensable especially in the region of transonic flow in which there is great interest today. The quasi-two-dimensional flow through compressor or turbine blading can be simulated by the flow through a plane CASCADE, i.e., by a row of blades having identical shapes and constant spacing along the blade height [1]. The cascade is used to divert a flow stream with an account of minimal loss. The turbine usually shows tolerance to the blade design and alignment errors because the blades of a turbine stage perform under a favorable pressure gradient while compressor blades are prone to aerodynamic losses because these have to work under adverse pressure gradients due to the diffusing nature of the flow field [2]. The blades of an axial compressor and axial turbine have high solidity which makes the flow structure in these machines highly complex as the flow around each blade is affected by the presence of the adjacent blades. These blades are therefore said to form a cascade [2,3]. The pressure ratio developed by a cascade depends on its aerodynamic characteristics. There are various types of shapes used in compressor blading. These range from the NACA series [4,5], C series, and DCA series. The aerodynamic parameters for compressor blades are camber, solidity, camber line shapes and thickness chord ratio. The peculiar geometry of their blades causes the flow to be three dimensional. The passage flow in

* Corresponding author.
E-mail address: satyam.panchal@uwaterloo.ca (S. Panchal).

http://dx.doi.org/10.1016/j.csite.2017.05.002
Received 17 February 2017; Accepted 7 May 2017
Available online 09 May 2017

Nomenclature

Re	Reynolds Number
Ma	Mach Number
S	Blade Pitch
l	Blade Chord (Actual Chord of Blade)
h	Blade Height
t	Blade Thickness
e	Axial Chord of Blade
C_P	Static Pressure Coefficient
NACA	National Advisory Committee for Aeronautics
DCA	Double Circular Arc

Greek symbols

α	Air Angle
β	Blade Angle
ν	Stagger Angle
θ	Camber Angle
i	Angle of incidence
δ	Deviation
$\in$	Fluid Deflection

these machines is entirely affected by pressure gradient, tip clearance, cross flows, secondary flows, and boundary layer effects [2,6]. Hence, understanding cascade flow is required, which results in systematic improvement of the aerodynamic art for design of these passages.

The heart of the design of an axial turbomachinery is the specification of a blade of an axial turbine or compressor. There have been many attempts to find solutions to these problems. A summary of these works have been discussed by Scholz [7], Roundbash [8], and Gostlow [9]. Compsty [10] has reported the work of Emery and Felix [11] in which it has been suggested that the shape of a compressor blade has an insignificant effect on its performance at low Mach numbers. Their tests on C4 and NACA65 series cascades revealed the same results. In another study, the flow development in S shaped profiles in a cascade tunnel was studied by Bacur [12]. Andrews [13] reported that the leading edge radius, the camber line shape and thickness chord ratio have a small effect on cascade performance. A detailed investigation of inter-passage flow in a baseline and modified versions of a two-stage axial compressor was carried out by Serovy et al. [14] and similarities in their aerodynamic performance was observed. In another study, Harrvey and Pullen [15] obtained a loading parameter for an axial flow turbine cascade by an accounting sweep of the blade. They did a validation of results with the experimental data of linear cascade tests of low pressure ratio axial turbines. Barrows et al. [16] tested cascades of varying aspect ratios between 1.5 and 3. Results of an off design performance of a turbine cascade at its mid span with varying Reynolds numbers, Mach numbers, and incidences were also studied by Mustaphe et al. [17]. Yamsaki et al. [18] developed a CFD code to compute unsteady aerodynamic forces on a vibrating annular cascade. They compared it with the linearized theory and they found the two to be almost similar. In another study, Basharat [2] constructed and tested an axial flat plate cascade for evaluating its aerodynamic performance. In his study, he found that the Reynolds number, incidence and blade angle of the cascade control the aerodynamic performance of the axial cascade. He also studied the variation of free stream velocity in the cascade tunnel, the variation of the angle of incidence with the blade angle, the variation of deviation angle, the variation of deflection angle, the variation of total pressure loss coefficient, the variation of static pressure rise coefficient, the variation of lift coefficient, and the variation of drag coefficient with blade angle and angle of incidence.

2. Experimental study

In this section, the experimental details are provided through the experimental set-up, air supply unit, inlet section, cascade blades, instrumentation of blade, cascade, and pressure probes.

2.1. Experimental set-up

The object is to study the behaviour of flow at the inlet, within the blade passage and at the exit of the compressor cascade. For this purpose, the flow is required to be surveyed at the inlet, within the blade passage and at the exit of the compressor cascade. To carry out systematic studies, a test rig was designed and fabricated. The schematic of experimental set up is shown in Fig. 1 and the picture of the experimental set up is shown in Fig. 2(A).

2.2. Air supply unit

The working fluid through the unit was air. A relatively large mass flow rate of air with pressure of few mm of water gauge was needed. A 2900 RPM blower was used to create such a flow. For the experimental a purpose blower with a cascade tunnel was used, after dismantling the cascade for experimentation. An impeller with backward curved vane, having suction pipe of diameter 270 mm and a discharge pipe of diameter 250 mm, was used. Flow control was achieved by a butterfly valve installed at the suction duct of the blower. For this experiment, the blower was operated at full throttle condition.

2.3. Inlet section

The uniform flow was to be achieved at the cascade inlet. This was done by using a settling chamber and contraction cone. The settling chamber was a rectangular tank into which the blower discharged the air. The contraction cone was used to make a uniform flow with minimum boundary layer effect. Both the contraction cone and setting chamber were fabricated from a M.S. (Mild Steel)

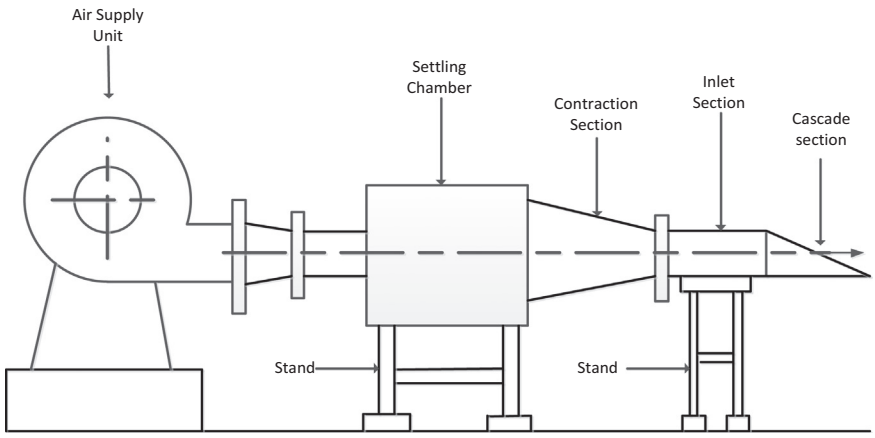

Fig. 1. Schematic of experimental set-up.

(A) Picture of experimental set-up

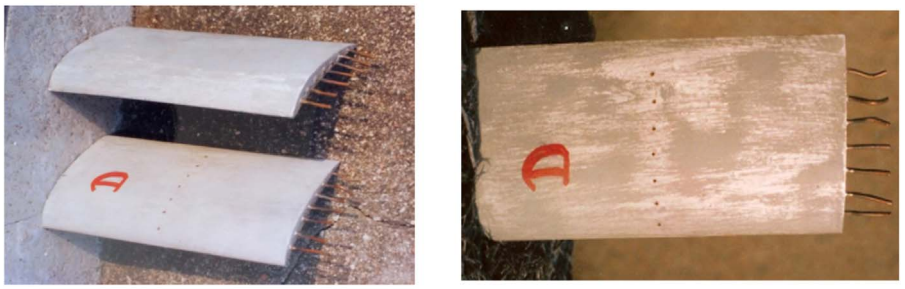

(B) Instrumented Blade

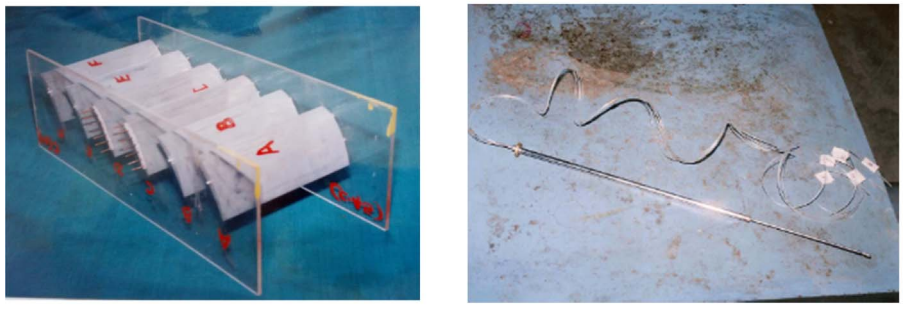

(C) Cascade Assembly **(D) Five hole Probe**

Fig. 2. Picture of experimental set-up, instrumented blades, cascade assembly, and five-hole probe.

sheet of 4 mm thickness. Air leakage through all joints was prevented using a rubber gasket of 5 mm thickness.

2.4. Cascade blades

The blades for the test cascade were made of aluminum using the casting method. The blades had a parabolic camber line and C4 base profile. These were mainly concerned with testing at low Mach number, 0.20–0.30 based on mean air conditions relative to the rotor and are thus more applicable for this experimental work. Other parameters for the test blades are shown in Table 1. A complete shape of an instrumented blade is shown in Fig. 2(B).

2.5. Instrumentation of blade

For measurement of static pressure distribution, the blade was instrumented with copper tubes of 0.75 mm diameter at various sections along the suction and pressure surface of the blade. Two blades, one for instrumentation on the pressure side and another for the suction side were used. Copper tubes were inserted in the blade mould before casting. Both ends of the copper tubes were open. One end was open at the blade surface and the other was projected through one of the side walls of the test section. Local static pressure on the blade surface was transmitted to the manometer through the open ends of the tubes. Fig. 2(B) shows a complete schematic of instrumented blades with the position of hypodermic tubes along the surface of the blade.

2.6. Cascade

A cascade was constructed by assembling a number of blades of a given shape and size at the required pitch and stagger angle as shown in Fig. 2(C). To analyse the flow, the cascade was fitted at the exit of the settling chamber, followed by the blower exit section. Various properties for the tested cascade are given in Table 2. For experimental purposes, a cascade was constructed by assembling 6 blades with the above mentioned data. The 3rd and 4th blades (see Fig. 2(C)) were instrumented for measurement of the blades' surface static pressure, one for measuring the suction side and the other for the pressure side.

2.7. Pressure probes

The five-hole probe used for measuring the flow quantities is shown in Fig. 2(D). Hypodermic stainless tubes of 0.9 mm outer diameter was used for the head construction. The sides, top and bottom of the tube were chamfered at 45° to their planes, because flow sensitivity of the tube is maximum at 45°. A probe generally used to give the local or spot condition. The overall condition may be different; hence it is necessary to take the probe reading at various points to survey velocity or pressure at that particular plane. This condition need to traverse the probe in axial, horizontal and vertical directions, which can be achieved by using the traversing mechanism. Similarly, to check the flow direction, it is necessary to have yaw movement in the flow passage. Therefore the probe was provided with three traversing mechanisms, horizontal movement, axial movement, and vertical and yaw movement mechanism. All the parts of the assembly were kept outside the flow field and only the 6 mm outer diameter probe stem was allowed inside the flow passage. The supporting frame structure, which was fixed to the ground matching its axis with the axis of the duct system, was fabricated and erected over the duct system. To prevent deformation and to maintain alignment with the duct system, the frame was welded with horizontal bars. The frame was fabricated from 25 mm diameter M.S. rod as shown in Fig. 2(A).

3. Measurements

As discussed in the experimental set up, the flow was supplied by the blower. The flow passed through the components of the rig and cascade. A detailed survey was made of total pressure, static pressure, velocity and flow direction and region of flow separation. Therefore the flow condition within the cascade, inlet and exit of the cascade was surveyed. As the expected flow was 3-dimensional in nature, a five-hole probe was used for the flow survey. For this, experimentation was carried out as for the incidences of –50°, −30°, −10° and 5°. The flow was surveyed by traversing the probe. A hole of 7 mm diameter was drilled at 350 mm before the cascade inlet which was about –500% times axial chord of the blade and the survey was carried out at all incidences. The flow was surveyed at the upstream of the cascade with the help of a 5-hole probe. The upstream position was at −17.5 mm before the leading

Table 1
Parameters of the test blades.

Item	value
Camber line	Parabolic
Base profile	C4
Position of maximum camber	40% of chord length from leading edge of the blade
Chord length	80 mm
Height of the blade	160 mm
Camber angle (Deflection)	45°
Stagger angle	30°

Table 2
Various design properties of the cascade.

Item	value
No. of blades	6
Length of the cascade	300 mm
Span of the cascade	160 mm
Pitch of the cascade	60 mm
Actual chord of the cascade	80 mm
Axial chord of the cascade	70 mm
Stagger angle of the cascade	30°
Pitch chord ratio	0.75

edge of the blade. This is equivalent to 25% of the axial chord of the blade. The flow was surveyed for one pitch distance (60 mm). The center to center distance between the two holes was 10 mm. In one pitch 7 holes were drilled, keeping in view the strength of the acrylic sheets. This was named plane A as show in Fig. 3.

It is necessary to know the flow conditions within the blade passages at various incidences. For surveying the flow, a number of holes were drilled in view of the size of the passage and the blockage effect. 5 holes were drilled along the pitch wise direction at the three axial positions. They were at 17.5 mm, 35.0 mm and 52.5 mm from the leading edge of the blade. They were at 25%, 50% and 75% of the axial chord of the blade. They were designated as plane B, Plane C and Plane D as presented in Fig. 3. To understand the flow conditions at the downstream of the cascade, 7 holes of equal size were drilled, covering one pitch distance (60 mm). The downstream position was at 105 mm from the leading edge of the blade. This was named plane E and is shown in Fig. 3. Table 3 indicates the positions of the various planes.

A five-hole probe of a head diameter 6 mm was traversed at all five planes (A to E) from the upstream to the downstream of the cascade. The probe was traversed along with the span wise direction from the side wall to a distance up to the mid span position ($z/h = 0.5$) and in the pitch wise direction covering one pitch at plane A and plane E and for the flow across the cascade passage framed by blade surveys at plane B, plane C and plane D between the pressure and suction surface, in order to determine the flow field within and along the blade passage. At each measuring location, the probe was nulled to make the pressure sensed by the yaw holes equal. The yaw angle and the pressure sensed by the five hole probe were recorded and the three components of velocity were determined using the calibration chart of the probe.

The measurement of pressure distribution on pressure and suction surfaces was carried out with the help of hypodermic tubes. They were located on the pressure and suction surfaces at 7 positions on each surface. Thus there were about 14 pressure tubes. The hypodermic tubes were located at the mid span of the blade and the pressure at these positions at various incidences was recorded with the help of a multitube manometer. The multitube manometer is shown in Fig. 2(A). A small amount of red ink was blended with water to facilitate the reading of the liquid in the manometer. There were about 24 tubes in the manometer.

4. Results and discussion

Using the five-hole probe, the observations were taken at different planes A, B, C, D and E at various incidences of −50°, −30°, −10° and 5°. From the observations, total pressure and velocity were determined. Holes of 7 mm diameter and 10 mm distance between the centres of two adjacent holes were drilled at these locations. The sizes of the holes were slightly higher than the size of

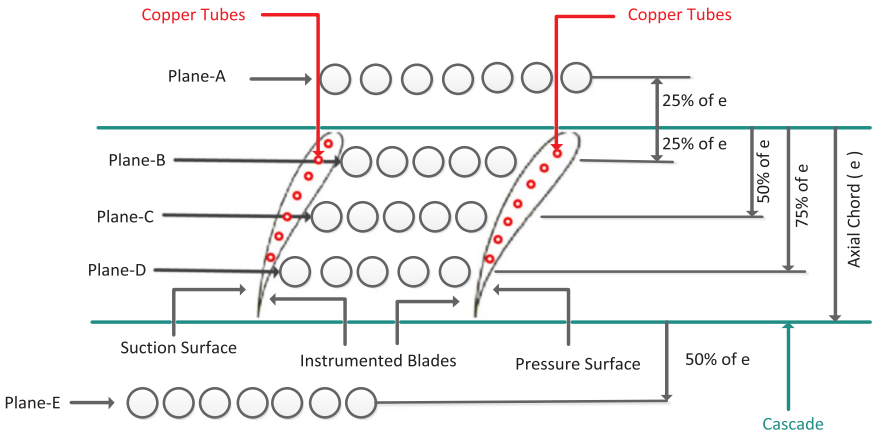

Fig. 3. Layout of Cascade.

Table 3
Position of various planes.

Plane	Position from leading edge in % of axial chord	No. of holes
A	−25% (−17.5 mm)	7
B	25% (17.5 mm)	5
C	50% (35 mm)	5
D	75% (52.5 mm)	5
E	150% (105 mm)	7

the probe to protect the probe from damage. The holes were blocked with rubber, which was inserted in to the holes. To prevent leakage while taking the observations, a sleeve was used with the probe.

4.1. Behaviour of flow far upstream of the cascade

The total pressure (P_0) along the span wise direction was measured for different incidences (I = −50°, −30°, −10° and 5°) far upstream of the cascade. The measured total pressure was non-dimensionalised by the average total pressure ($\overline{P_0}$). The span wise distance was non-dimensionalised by the total height of the blade (z/h). The variation of the upstream side total pressure ($P_0/\overline{P_0}$) with the span wise non-dimensional distance (z/h) is shown in Fig. 4(A). From the graph, it is clear that the flow was almost uniform at the inlet with constant total pressure. Slight variations were noticed near the end walls because of the growth of the boundary layer. The total pressure profiles were observed to be similar for different incidence angles without any upstream effects of the cascade leading edge. Fig. 4(B) shows the variation of velocity far upstream of the cascade. The velocity remains almost constant near the mid span of the cascade but there is very little reduction in velocity near the walls because of the boundary layer effect. Similarly, the effect of the flow angle far upstream of the cascade was studied, and it was found that the flow was almost in the axial direction of the duct.

4.2. Behaviour of flow upstream of the cascade (plane A)

The flow conditions in terms of total pressure were measured and plotted in Fig. 5(A) and Fig. 5(B). The total pressure distribution along various span wise positions are plotted along one pitch distance (60 mm) at various incidences. The distribution is shown at 20 mm, 40 mm, 60 mm and 80 mm from the tip of the blade of the cascade. This is also at 12.5%, 25%, 37.5% and 50% (mid span position) of the total blade height. The total pressure is plotted in terms of mm of water and the experiment was conducted at all incidences of I = −50°, −30°, −10°and 5°. Fig. 5(A) and Fig. 5(B) show the plot of I = −50° and −30° incidences at 50% and 12.5% of the blade height. The plot shows that the total pressure distribution of the flow along the pitch remains almost constant. This was observed at all span positions. The flow conditions were found to be the same at all incidences and were therefore not plotted for I = −10° and 5°.

The velocity distribution plotted against one pitch distance (60 mm) for various incidences is shown in Fig. 5(C) at mid span position. The velocity plot shows slight lower velocity near to the wall and higher velocity at the mid span position. The variation in velocity in every span position along the pitch is much less. A higher variation in velocity is observed at −50° incidence at all span positions. Similar plots have been made for 12.5%, 25%, and 37.5% of the total blade height at incidences of I = −50°, −30°, −10°and 5° and Fig. 5(D) shows the velocity distribution of flow at 12.5% of blade height at various incidences at plane A.

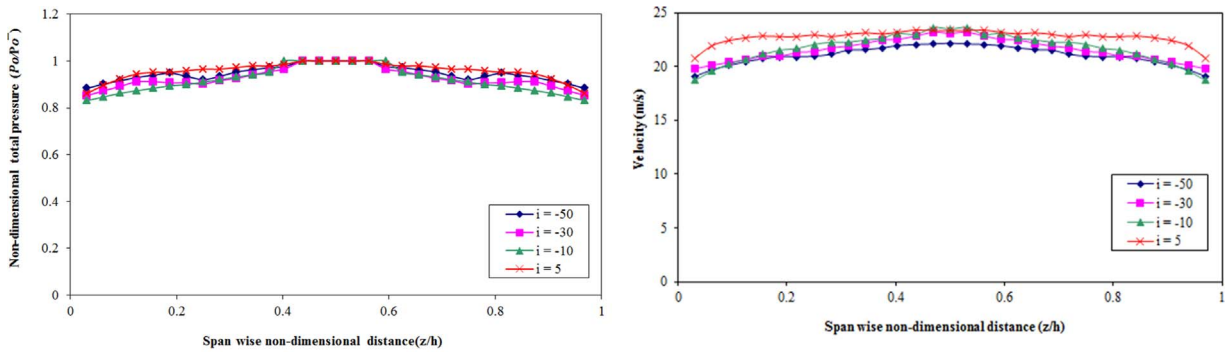

(A) Span wise variation of total pressure at far upstream of the cascade

(B) Span wise variation of velocity at far upstream of the cascade

Fig. 4. Span wise variation of total pressure and velocity at far upstream of the cascade.

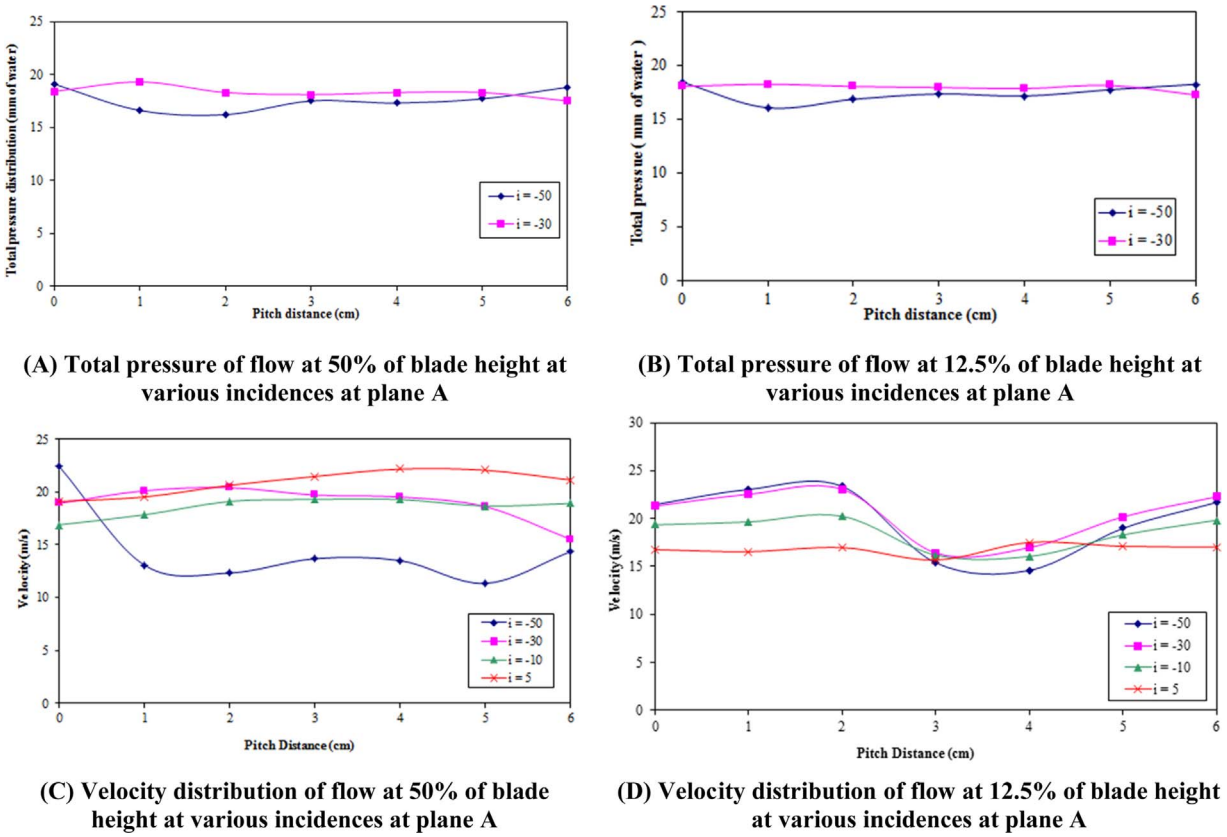

Fig. 5. Total pressure of flow at 50% and 12.5% of blade height at various incidences at plane A.

4.3. Behaviour of flow within the cascade (Plane B, C, and D)

The behaviour of flow was studied within the cascade passage (planes B, C, and D) shown in Fig. 3 at 25%, 50% and 75% of the axial chord of blade. It was found that at I = −50° at plane B there was increase in the velocity of the flow. The same trend was also observed at plane C. Thereafter, there was a decrease in velocity at plane D. The flow velocity was lower near the pressure surface and higher near the suction surface. There was a significant flow disturbance near the pressure surface from the leading edge to the trailing edge. This was a growth in the disturbed flow region from the leading edge to the trailing edge. The trend was the same at 12.5%, 25%, 37.5% and 50% (mid span position). The observed velocity vector showed that there was less flow turning towards the suction surface compared to the pressure surface.

The velocity pattern was changed with –30° incidence compared with –50° incidence. The disturbed region of the flow was found near to plane B in the vicinity of the pressure surface. After plane B, the flow was well distributed within the passage, velocity again was found to be less near to the pressure surface compared to the suction surface. The same trend is noticed at all span positions. The same trend was observed at –10° incidence but at 5° incidence, the flow disturbance on account of rotational flow was found to disappear. The velocity was almost the same near the pressure surface and within the passage at all planes. This was found at all span wise positions.

4.4. Behaviour of flow downstream of the cascade (Plane E)

The total pressure distribution of the flow at various incidences along the pitch for mid span positions is shown in Fig. 6(A) which shows that the lower value of the pressure occurs near the pressure surface. This is roughly at about 60% of the pitch. The pressure is higher towards the suction surface. A large variation in pressure is observed at −50° and −30° incidences. A minimum variation of total pressure is found at 5° incidence. The same trend is observed for all span positions and Fig. 6(B) shows the total pressure of flow at 12.5% of blade height at various incidences at plane E. The velocity distribution of the flow at various incidences for the mid span position is shown in Fig. 6(C). The velocity distribution shows that there is a large variation in velocity at −50° and −30° incidences. There is minimum variation in velocity at −10° and 5° incidences. The same trend is observed for all span positions and Fig. 6(D) shows the velocity distribution of flow at 12.5% of blade height at various incidences at plane E.

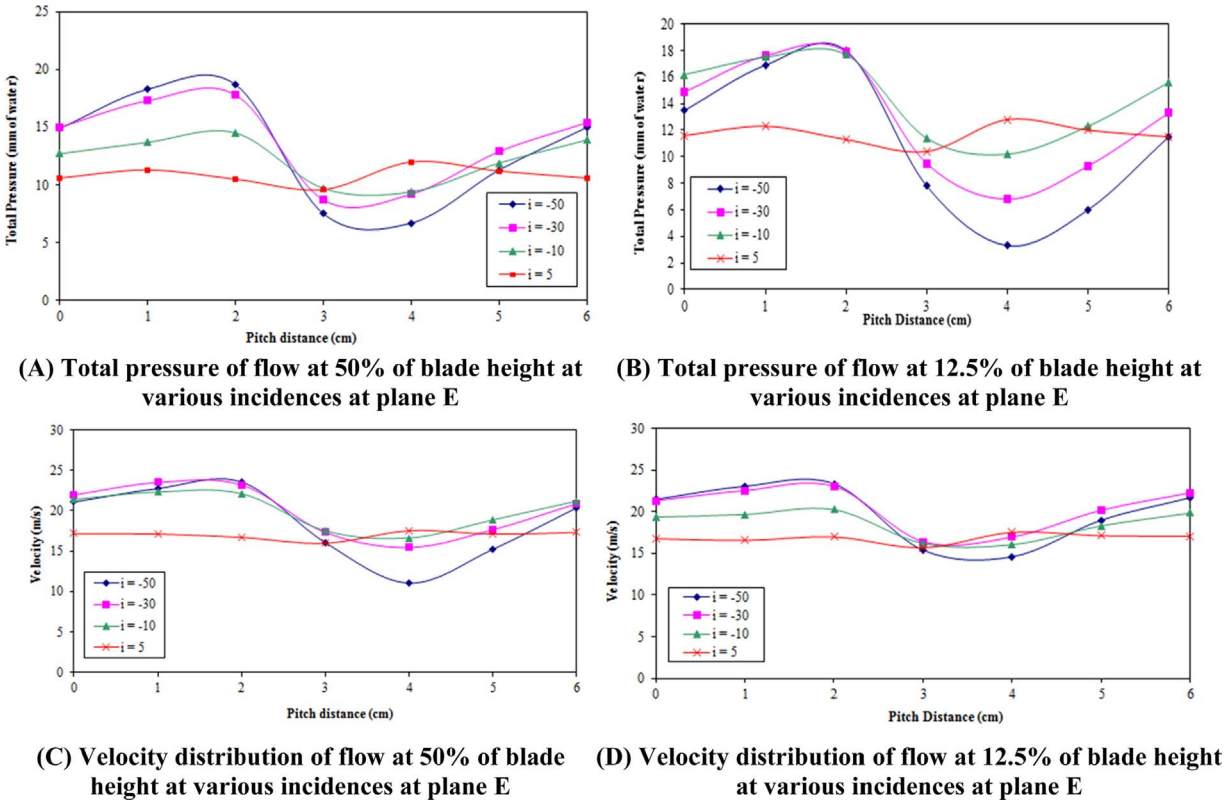

Fig. 6. Total pressure of flow at 50% and 12.5% of blade height at various incidences at plane E.

4.5. Blade surface pressure distribution

The blade surface pressure distribution is analyzed in form of static pressure coefficient which is defined

$$C_P = (P_s - P_{s0})/\frac{1}{2}\rho V_0^2 = (P_s - P_{s0})/(P_{t0} - P_{s0}) \quad (1)$$

Where, C_P is the static pressure coefficient on the pressure surface and suction surface, P_s is the static pressure on the surface of the blade, P_{s0} is the static pressure far upstream of the cascade, P_{t0} is the total pressure far upstream of the cascade, ρ is density of air, and V_0 is span wise average velocity far upstream of the cascade. Fig. 7(A) and Fig. 7(B) show comparison of static pressure distribution on the pressure surface and suction surface at various incidences (I = −50°, −30°, −10° and 5°) against non-dimensional chord length (x/l).

From Fig. 7(A), it is clear that at incidence angle of −50°, there is initial diffusion from the leading edge of the blade to up to 25%

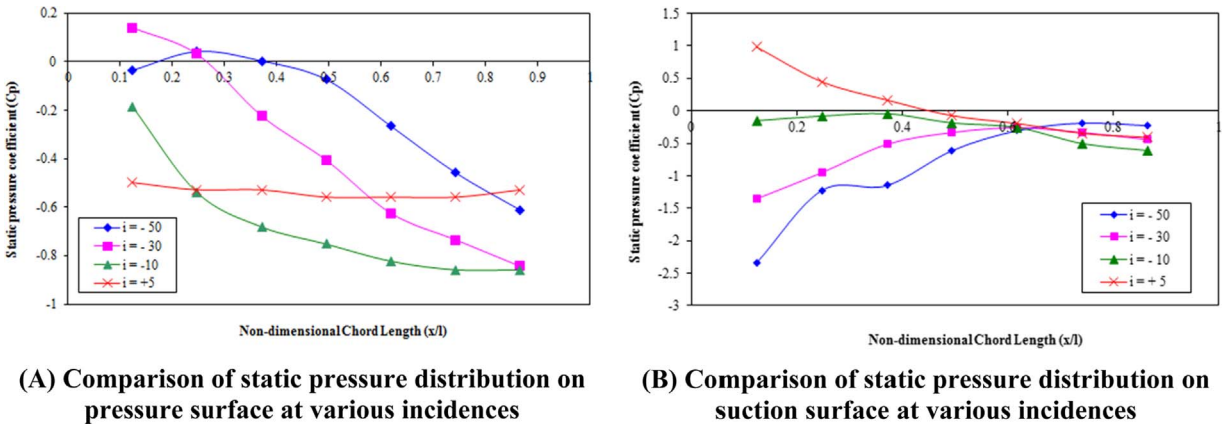

Fig. 7. Comparison of static pressure distribution on pressure and suction surface at various incidences.

of the axial chord of blade and after that there is acceleration for the remaining part of the blade, while at -30° incidence there is continuous acceleration from the leading edge to the trailing edge. At -10° incidence, there is acceleration up to about 75% of the axial chord and thereafter it remains constant. For an incidence angle of 5°, pressure distribution remains almost constant from the leading edge to the trailing edge.

Fig. 7(B) shows there is continuous diffusion on the suction surface from the leading edge to up to about 63% of the axial chord from the leading edge for incidences of -50° and -30°. For -10° incidence there is a very low rate of diffusion up to 40% of the axial chord and then continuous acceleration, while for 5° incidence there is continuous acceleration from the leading edge to the trailing edge of the blade. After 63% of the axial chord from the leading edge, the pressure distribution remains constant for all incidences up to the trailing edge of the blade.

5. Conclusions

The objective of this work was to study the behaviour of flow at the inlet, within the blade passage and at the exit of the compressor cascade. For this, a cascade was constructed with six aerofoil blades, out of which two were instrumented blades. Aerodynamic performance of the cascade was evaluated. From the experiments, the following conclusions can be made. 1) at far upstream of the cascade, there was less effect of incidence on the flow parameters, 2) The incidence affected the flow parameters and flow directions upstream of the cascade, 3) At higher negative incidence, there was a greater disturbance on the flow conditions within the cascade passage. The disturbances were very high near to the pressure surface. With positive incidence, the disturbance decreased near to the pressure surface, 4) There were no disturbances with any incidences in the region near to the suction surface, 5) The pressure distributions on the pressure surface, as well as suction surface, were affected by the flow incidence. The effect of incidence was greater on the pressure surface. Continuous deceleration was observed on the suction surface at higher negative incidence, 6) The effect of incidence failed at roughly about 50% of the axial chord on the suction surface; i.e. the incidence very much affected the pressure distribution on the pressure and suction surfaces on the leading edge of the blade, 7) A wake was formed on the pressure surface side compared to the suction surface side. The magnitude of the wake was very high at –50° incidence. The wake reduced with increase in incidence.

Terms and definitions

Pitch-Chord Ratio	s/l	Ratios of the blade pitch to the blade chord [19].
Mach Number	M	The ratio of the speed of a body to the speed of sound in the surrounding medium. M = 2 to 2.5 for axial turbo machines [20].
Solidity	σ = l/s	The solidity (σ = l/s) the ratio of chord to pitch, reciprocal of pitch-chord ratio [15].
Aspect Ratio	h/l	The aspect ratio (h/l) is the ratio of the blades height to the blade length
Leading Edge	L.E.	At inlet to an aerofoil blade, there is a thick rounded curved portion, which is called the leading edge where the flow approaches the blade.
Trailing Edge	T.E.	At exit of an aerofoil blade there is a sharp portion called the trailing edge where the flow leaves the blade.
Chord line & Chord Length	l	A straight line joining the leading edge and the trailing edge is known as a chord line and the distance between the leading edge and the trailing edge is known as chord length. It is denoted by (l).
Camber Line	–	A blade section of an infinitesimal thickness is a curved line joining the leading edge (L.E) and trailing edge (T.E), known as the “camber line”.
Camber Angle	θ	Camber angle is an angle between the chord line and tangent to the camber line.
Blade Angle	β	The blade angle is an angle between the axial direction and the tangent to the camber line.
Air Angle	α	Air angle is defined as an angle between the axial direction and the flow direction.
Stagger Angle	ν	Stagger angle is the angle between the chord line and axial direction.
Angle of incidence	i	The difference between the air angle (α_1) and the blade angle (β_2) at entry is known as the angle of incidence.
Deviation	δ	The deviation is defined as the difference between the air angle and blade angle at exit.
Fluid Deflection	$\in$	Fluid deflection is defined as the difference between air angles at the inlet and outlet

References

[1] S. Yahya, Turbine, Compressors & Fans, 4TH ed, Tata McGraw Hill, 2011.
[2] S. Basharat, Performance of an axial cascade, J. Fluid Dyn. no. 3 (2013) 191–197.
[3] R. Gerald, J. Friedrichs, Procedure for Analyzing, Manipulating and Meshing of Compressor blades to simulate their flow, Int. J. Gas. Turbine Propuls. Power Syst. 8 (1) (2016).
[4] G. Medic, V. Zhang, G. Wang, J. joo, O.P. Sharma, Prediction of transition and losses in Compressor cascades using large-eddy simulation, ASME: J. Turbomach. 138 (12) (2016) 121001–121009.
[5] M. Böhle, T. Frey, Numerical and experimental investigations of the three- dimensional-flow structure of tandem cascades in the sidewall region, J. Fluids Eng. 136 (7) (2014) (071102-1-071102-13).

[6] N. Smith, W. Murray III, N. Key, Considerations for measuring compressor aerodynamic excitations including Rotor wakes and tip leakage flows, J. Turbomach. 138 (3) (2016) (031008-031008-9).
[7] N. Scholz, Aerodynamics of Cascades, Nato Science and Technology Organization, Amsterdam, 1977.
[8] W. H. Roundebush, Potential Flow in Two Dimensional Cascades, Chapter IV of 'Aerodynamic Design of Axial Flow Compressors', NASA Sp 36, US Government Printing Office, Washington DC, 1965.
[9] J.P. Gostlow, Cascade Aerodynamics, Pergaman Press, Oxford, 1984.
[10] N.A. Cumpsty, Compressor Aerodynamics, Longman Scientific and Technical, England, 1989.
[11] A. Felix, J. Emery, A Comparison of Typical NGTE and NACA Axial Blade Compressor Blade Sections in Cascades at Low Speeds, US Government Printing Office, Washington DC, 1957 (in NACA TN 3937).
[12] I. D. Baciu, A S Profile axial cascade tested in a wind tunnel, International Conference on Hydraulic Machinery and Equipment, vol. Timosoars, 16–17 October 2008, pp. 45-48.
[13] S.J. Andrew, Tests Related to the Effect of Profile Shape and Camber-Line on Compressor Cascade Performance, Aeronautical Research Council R & M 2743, England, 1949.
[14] G. Serovy, P. Kavanagh, T. Okishi, Aerodynamics of Advanced Axial Turbomachinery, US Government Printing Office, Washington DC, 1983 (in NTIS Report ADA 131360).
[15] G. Pullen, N. Harrvey, Influence of sweep on the axial flow turbine cascade at Mid span, Trans. ASME, J. Turbomach. 129 (3) (2007).
[16] D. Kalpatrik, R. Burrow, Aspect Ratio Effects on Compressor Cascade Blade Flutter (ARC Technical Report), Aeronautical Research Council, England, 1958 (R & M No. 3103).
[17] H. Mustaphe, D. Jourim, S.A. Scolander, Aerodynamic performance of a transonic turbine cascade at off design conditions, J. Turbomach. 123 (3) (2001) 510–519.
[18] T. Nagasaki, N. Yamasaki, Linear Unsteady aerodynamic forces on a vibrating annular cascade blade, J. Therm. Sci. 12 (2) (2003) 138–143.
[19] E.T. Vincent, The Theory and Design of Gas Turbines and Jet Engines, McGraw Hill, New York, 1950.
[20] A.S. Ucer, P. Stow, C.H. Hirsch, Thermodynamic and Fluid Mechanics of Turbomachinery Volume I & II, Martinus Nijhoff, In Corporation with NATO Scientific Affairs Division, Boston, 1985.